

Stable structures and superconductivity of Ca-As-H system under high pressure

Lanci Guo(郭兰慈), Qiyue Zhang(张启悦), Yuechen Guo(郭悦晨), Gang Chen(陈刚), and Jurong Zhang(张车荣)
Citation: Chin. Phys. B, 2025, 34 (**11**): 117401. DOI: 10.1088/1674-1056/ae00ac
http://cpb.iphy.ac.cn; http://iopscience.iop.org/cpb

What follows is a list of articles you may be interested in

Pressure-stabilized Li_2K electride with superconducting behavior

Xiao-Zhen Yan(颜小珍), Quan-Xian Wu(邬泉县), Lei-Lei Zhang(张雷雷), and Yang-Mei Chen(陈杨梅)
Chin. Phys. B, 2025, 34 (**9**): 097405. DOI: 10.1088/1674-1056/add009

Superconductivity and band topology of double-layer honeycomb structure M_2N_2 (M = Nb, Ta)

Jin-Han Tan(谭锦函), Na Jiao(焦娜), Meng-Meng Zheng(郑萌萌), Ping Zhang(张平), and Hong-Yan Lu(路洪艳)
Chin. Phys. B, 2025, 34 (**9**): 097402. DOI: 10.1088/1674-1056/adee04

Surface reconstruction modulated superconductivity on quasi-2D iron pnictide superconductor $KCa_2Fe_4As_4F_2$

Wenjing Zeng(曾文静), Zongyuan Zhang(张宗源), Xiaoyan Dong(董晓燕), Yubing Tu(涂玉兵), Yanwei Wu(吴彦玮), Teng Wang(王腾), Fan Zhang(张凡), Shuai Shao(邵帅), Jie Hou(侯杰), Xingyuan Hou(侯兴元), Ning Hao(郝宁), Gang Mu(牟刚), and Lei Shan(单磊)
Chin. Phys. B, 2025, 34 (**8**): 087402. DOI: 10.1088/1674-1056/add5cb

Superconductivity in YbN_4H_{12} under low pressures

Xiang Wang(汪翔), Chenlong Xie(谢晨龙), Haohao Hong(洪浩豪), Yanliang Wei(魏衍亮), Zhao Liu(刘召), and Tian Cui(崔田)
Chin. Phys. B, 2025, 34 (**8**): 087401. DOI: 10.1088/1674-1056/add908

Theoretical investigation of potential superconductivity in Sr-doped $La_3Ni_2O_7$ at ambient pressure

Lei Shi(石磊), Ying Luo(罗颖), Wei Wu(吴为), and Yunwei Zhang(张云蔚)
Chin. Phys. B, 2025, 34 (**7**): 077403. DOI: 10.1088/1674-1056/add1bd

---

SPECIAL TOPIC — Structures and properties of materials under high pressure

Stable structures and superconductivity of Ca–As–H system under high pressure

Lanci Guo(郭兰慈), Qiyue Zhang(张启悦), Yuechen Guo(郭悦晨), Gang Chen(陈刚)[†], and Jurong Zhang(张车荣)[‡]

School of Physics and Electronics, Shandong Normal University, Jinan 250014, *China*

(Received 9 June 2025; revised manuscript received 8 August 2025; accepted manuscript online 29 August 2025)

Obtaining room-temperature superconductors has long been a research hotspot in the field of condensed matter physics. Previous studies have shown that doping strategies can effectively enhance the superconducting properties of materials. In this work, we employed first-principles calculations combined with the particle swarm optimization method to explore the structural possibilities of the Ca-doped As–H ternary system and to calculate the electronic and superconducting properties of the newly identified structures. Two thermodynamically stable hydrides were found under high pressure. The *P*4/*nmm*-Ca_2AsH_4 phase remains thermodynamically stable within the pressure range of 90–200 GPa, while the *Cc*-Ca_2AsH_6 phase exhibits stability over a broader range of 79–200 GPa. Electron-phonon coupling analysis indicates that the superconducting critical temperatures (T_c) of *P*4/*nmm*-Ca_2AsH_4 and *Cc*-Ca_2AsH_6 are 11 K and 16 K at 100 GPa, respectively. The incorporation of Ca significantly reduces the thermodynamic stability pressure of As–H compounds with higher hydrogen content, thereby improving their synthetic accessibility.

Keywords: superconductivity, first-principles calculations, hydrogen-rich compounds

PACS: 74.62.Fj, 74.20.Pq, 74.25.Kc, 63.20.dk

DOI: 10.1088/1674-1056/ae00ac **CSTR:** 32038.14.CPB.ae00ac

1. Introduction

The investigation of room-temperature superconductors under high-pressure conditions represents a pivotal area of research in condensed matter physics. Based on the Bardeen–Cooper–Schrieffer (BCS) theory[1] and supported by experimental advancements in high-temperature superconductivity, hydrogen-rich compounds exhibiting remarkably high superconducting critical temperatures (T_c) have been identified in recent years. Notable examples include LaH_{10},[2–5] which demonstrates a T_c of 260 K at 170 GPa, and H_3S,[6,7] which achieves 200 K at 160 GPa. Moreover, hydrogen-rich compounds such as CaH_6,[8,9] YH_6,[2,3,10,11] and YH_9,[2,3,10,11] have been successfully synthesized under experimental conditions and have demonstrated exceptional T_c values. Recent breakthroughs in the discovery of room-temperature superconductors, along with advancing theoretical insights into the phonon-mediated mechanisms of hydrogen-rich compounds, have significantly accelerated the exploration of novel hydrogen-rich superconducting materials.[12–14] Ternary hydrides, characterized by their enhanced configurational degrees of freedom, exhibit more complex chemical compositions and diversified crystal structures compared to conventional binary hydrides.[14] Consequently, they hold the potential to manifest a broader range of novel physicochemical properties. The metastable ternary hydride Li_2MgH_{16},[15] obtained by doping lithium into the binary hydrogen-rich compound MgH_{16}, exhibits a T_c significantly exceeding room temperature under high pressure. Beryllium-doped $LaBeH_8$[16] achieves a T_c of 110 K at a relatively moderate pressure of 80 GPa, representing a considerable reduction in the required pressure compared to undoped LaH_{10}.

The arsenic–hydrogen (As–H) compound AsH_3 is thermodynamically stable at low pressures, yet its electronic structure exhibits semiconducting behavior.[17] Previous investigations have indicated that As–H compounds could achieve remarkably high T_c values under extreme pressures exceeding 300 GPa.[18] The metastable AsH_2[19] exhibits a T_c of 81 K at 200 GPa, and the *C*2/*c* phase of AsH_8[18] attains a T_c of 152 K at 450 GPa, significantly surpassing the liquefaction temperature of nitrogen (77 K). As a representative of the alkaline earth elements, calcium-based hydrides have achieved substantial advancements in various aspects. Fascinating structures such as $CaAlH_7$ ($\sim$ 53 K at 150 GPa),[20] Ca_3CeH_{24} ($\sim$ 175 K at 200 GPa),[21] $CaYH_6$ ($\sim$ 61 K at 0.001 GPa),[22] $CaYH_8$ ($\sim$ 90 K at 100 GPa),[22] $CaYH_{10}$ ($\sim$ 109 K at 100 GPa),[22] $CaYH_{12}$ ($\sim$ 226 K at 150 GPa),[22] and Ca_2SnH_{18} ($\sim$ 111 K at 110 GPa)[23] exhibit remarkable T_c values under pressures below 300 GPa. Inspired by these prior studies, we introduced Ca doping into As–H compounds to design Ca–As–H ternary systems capable of stabilizing under moderate pressure conditions.

[†]Corresponding author. E-mail: phdgchen@163.com

[‡]Corresponding author. E-mail: zjr@calypso.cn

© 2025 Chinese Physical Society and IOP Publishing Ltd. All rights, including for text and data mining, AI training, and similar technologies, are reserved.

In this study, we systematically investigated the Ca–As–H system under different pressure conditions by first employing the CALYPSO code[24,25] to predict stable crystal structures, followed by first-principles calculations to evaluate their stability and physical properties.[22,26–31] By incorporating the alkaline earth element Ca into the As–H system, we successfully reduced the stabilization pressure of binary As–H hydrides with higher hydrogen stoichiometry. Our investigation revealed that the *P*4/*nmm*-Ca_2AsH_4 and *Cc*-Ca_2AsH_6 phases exhibit metallic behavior within a moderate pressure range.

2. Results and discussion

Figure 1 presents the convex hull of the Ca–As–H ternary system, constructed through an in-depth thermodynamic investigation of its associated unary and binary compounds. Previous studies have extensively documented the pressure-induced phase transitions of Ca,[32–34] As,[35] and H.[36] The structural and superconducting characteristics of specific binary hydrides in the Ca–H[8,37] and As–H[18,19] systems have been further confirmed by recent investigations. For the Ca–As subsystem, this ternary study focused on stoichiometric ratios of 1:1 and 2:1 for Ca and As. A comprehensive structural search at 100 GPa and 200 GPa identified two stable phases: CaAs with the *P*4/*mmm* structure and Ca_2As with the *P*6/*mmm* and *P*6_3/*mmc* structures. In the ternary Ca–As–H system, two compounds — *P*4/*nmm*-Ca_2AsH_4 and *Cc*-Ca_2AsH_6 — were identified as thermodynamically stable structures at both 100 GPa and 200 GPa.

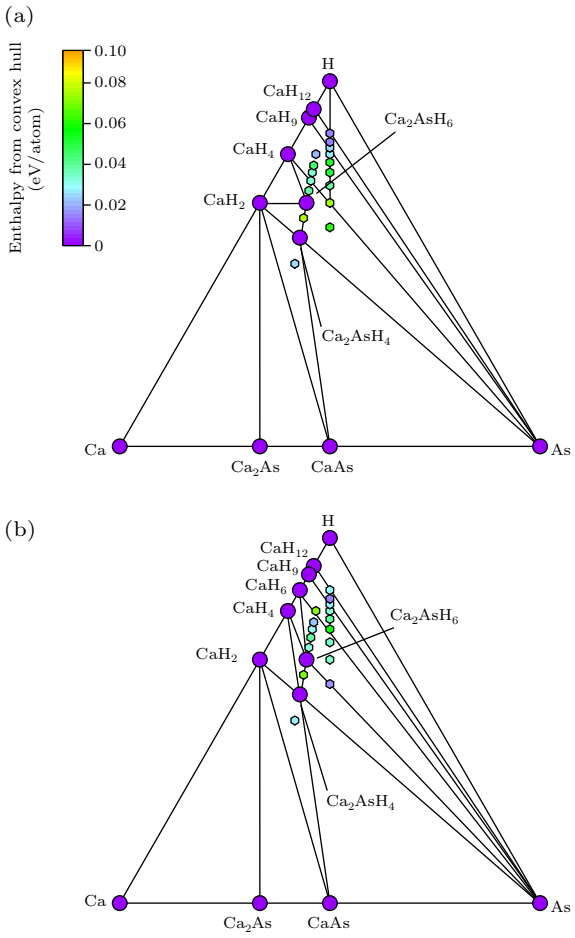


Fig. 1. Calculated phase stabilities of the Ca–As–H system relative to Ca, As, H, and their binary compounds at (a) 100 GPa and (b) 200 GPa. The purple dots denote the stoichiometries that are thermodynamically stable, whereas the colored dots represent metastable phases.

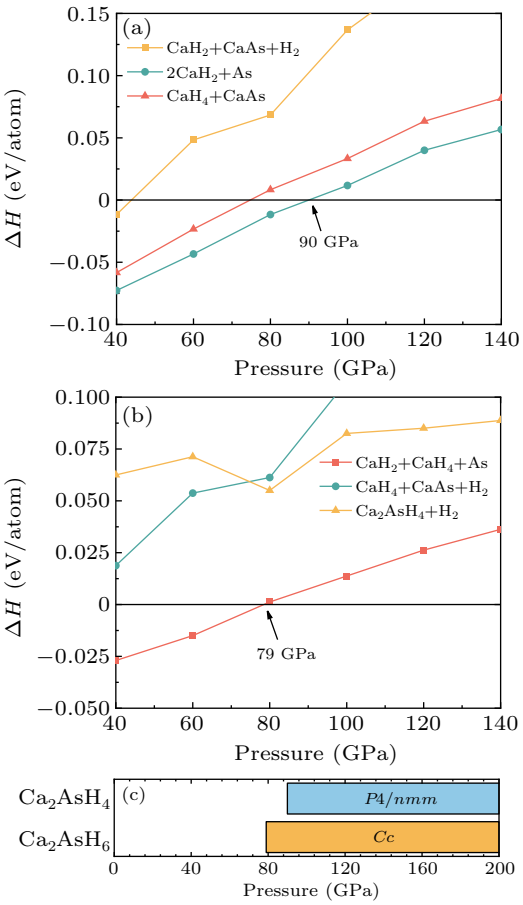


Fig. 2. (a) and (b) The relative enthalpies of various structural candidates for Ca_2AsH_4 and Ca_2AsH_6, respectively. In (a), the enthalpy of the *P*4/*nmm*–Ca_2AsH_4 phase is taken as the reference (0 eV), whereas in panel (b), the *Cc*–Ca_2AsH_6 phase serves as the reference. The enthalpy differences (ΔH) are plotted in eV per atom as a function of pressure. The colored curves represent different decomposition pathways, as indicated in the legends. (c) The predicted pressure–composition phase diagram for Ca_2AsH_4 and Ca_2AsH_6.

To explore the possible synthesis pathways of *P*4/*nmm*-Ca_2AsH_4 and *Cc*-Ca_2AsH_6, we plotted a pressure–enthalpy phase diagram, as shown in Fig. 2. For *P*4/*nmm*-Ca_2AsH_4, we examined three potential decomposition pathways (CaH_2 + CaAs + H_2, $2CaH_2$ + As, and CaH_4 + CaAs), as illustrated in Fig. 2(a). Our analysis indicates that *P*4/*nmm*-Ca_2AsH_4 becomes thermodynamically stable above 90 GPa and is most likely synthesized from a high-pressure reaction between CaH_2 and As. For *Cc*-Ca_2AsH_6, we investigated three possible decomposition pathways (CaH_2 + CaH_4 + As, CaH_4 + CaAs, and Ca_2AsH_4 + H_2), as shown in Fig. 2(b). Our findings suggest that *Cc*-Ca_2AsH_6 begins to stabilize above 79 GPa and is most likely synthesized from a mixture of CaH_2, CaH_4, and As under high pressure. We also calculated

the phonon dispersion relations of these two phases to evaluate their dynamic stability, as shown in Fig. 5. The absence of imaginary frequencies across the Brillouin zone confirms that both phases are dynamically stable at their corresponding pressures. Based on the above results, we plotted the stability ranges for these two phases, as shown in Fig. 2(c).

The crystal structures of *P*4/*nmm*-Ca_2AsH_4 and *Cc*-Ca_2AsH_6 are illustrated in Fig. 3. For *P*4/*nmm*-Ca_2AsH_4 at 100 GPa, H and Ca atoms form two types of coordination units: CaH_6 and CaH_9, with As atoms distributed around these units. The shortest H–H distance is 1.83 Å. In contrast, *Cc*-Ca_2AsH_6, which crystallizes in a lower-symmetry space group, exhibits structural motifs featuring quasi-molecular H_2 units.[36] These H–H pairs can be classified into two categories according to bond length, with distances of approximately 0.90 Å (H_2_s) and 0.95 Å (H_2_l). In addition, several isolated H atoms (H_iso) are distributed within the lattice. Detailed crystallographic parameters are presented in Table S1.

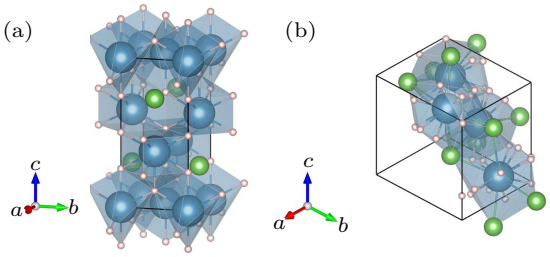


Fig. 3. Crystal structures of (a) *P*4/*nmm*-Ca_2AsH_4 and (b) *Cc*-Ca_2AsH_6 at 100 GPa. Ca, As, and H atoms are shown as blue, green, and pink spheres, respectively.

As part of our bonding analysis, we calculated the electron localization function (ELF) for both phases, as shown in Fig. S1, with the isosurface value set to 0.7. In *P*4/*nmm*-Ca_2AsH_4 at 100 GPa, the ELF isosurfaces formed between H atoms adjacent to As atoms exhibit distinct directional characteristics, indicating the presence of polar covalent bonds, similar to those observed in covalent hydride superconductors such as H_3Se.[38,39] In contrast, Ca atoms and some H atoms display significant localization.

For *Cc*-Ca_2AsH_6, the situation is more complex due to its low symmetry. Four isolated H atoms, two pairs of H_2 molecular units, and two pairs of As–H_2 covalent groups are dispersed within the lattice. The As–H_2 covalent groups consist of As atoms bonded to adjacent H_2_s units. To further understand the electronic charge distribution, a Bader charge analysis was performed, and the results are summarized in Table S2. In the Ca–As–H system, the analysis reveals that Ca acts as an electron donor, whereas both As and H act as electron acceptors. For *P*4/*nmm*-Ca_2AsH_4 at 100 GPa, each Ca atom donates approximately 1.03*e*, while each As atom gains 0.36*e*. The H atoms can be divided into two categories according to their coordination environments: one group gains 0.54*e*, and the other slightly less, 0.31*e*.

For *Cc*-Ca_2AsH_6, each Ca atom donates 1.03*e* as well, but the number of electrons acquired by each As atom increases markedly to 0.64*e*. Among the hydrogen species, each H_2_s unit gains approximately 0.29*e*, the H_2_l unit gains approximately 0.31*e*, and each H_iso atom gains around 0.42*e*. For As–H compounds,[18] such as *C*2/*m*–AsH_8, each H atom gains roughly 0.1*e*, with a nearest H–H bond length of 0.8 Å at 350 GPa. The electron gain per H atom in Ca–As–H systems at 100 GPa is therefore higher, accompanied by longer H–H bond distances. Ca doping enhances the electron acceptance of H atoms, significantly extending the H–H bond length and improving the structural stability.[40,41]

As shown in Fig. 4, the coexistence of conduction and valence bands at the Fermi level in both *P*4/*nmm*-Ca_2AsH_4 and *Cc*-Ca_2AsH_6 indicates their metallic nature. Meanwhile, both phases exhibit strong hybridization below the Fermi level. For *P*4/*nmm*-Ca_2AsH_4, no apparent flat bands are observed near the Fermi level, but a distinct Dirac cone[42] appears along the *M*–*Γ* direction. The density of states (DOS) at the Fermi level is dominated by Ca, with H contributing only a small fraction. In contrast, *Cc*-Ca_2AsH_6 displays relatively flat bands, suggesting that the electrons possess higher effective mass and lower carrier mobility.[43] The DOS at the Fermi level is mainly contributed by As, with nearly equal contributions from Ca and H. For comparison, in *C*2/*m*–AsH_8 at 350 GPa, the DOS near the Fermi level is primarily derived from H electrons. Overall, the low H-DOS at the Fermi level explains the relatively low T_c values predicted for both phases.[12,14]

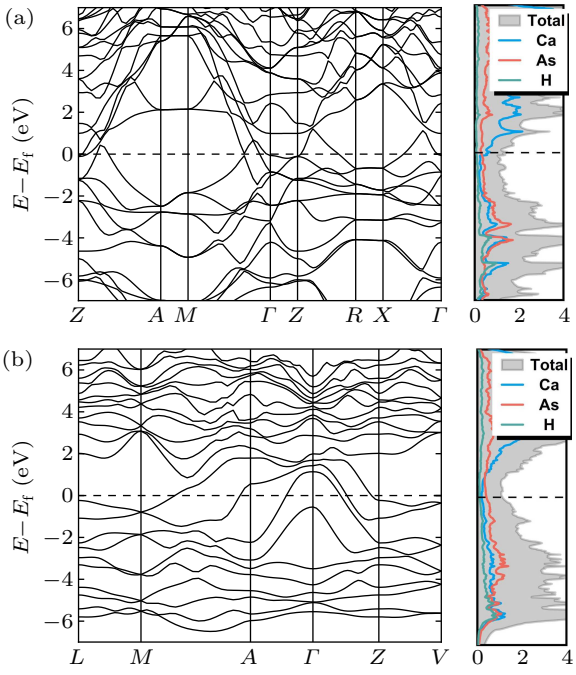


Fig. 4. Electronic band structures and projected densities of states for (a) *P*4/*nmm*-Ca_2AsH_4 and (b) *Cc*-Ca_2AsH_6 at 100 GPa. The Fermi energy (black dashed line) is set to zero.

To evaluate the superconducting behavior of the Ca–As–H system, we performed comprehensive calculations involv-

ing the DOS at the Fermi level N_{Ef}, the electron–phonon coupling (EPC) parameter λ, and the logarithmic average phonon frequency ω_{log}. Recognizing the significance of the Coulomb pseudopotential μ^*, particularly given that all calculated λ values are less than 1.5, we set $\mu^* = 0.10$ and 0.13 to refine our estimates of the superconducting transition temperature T_c.[15,44,45] A detailed summary of the computed parameters and corresponding T_c values is presented in Table 1.

Table 1. Key superconducting parameters for Ca–As–H compounds are listed. The T_c of two phases are calculated with $\mu^* = 0.1$ and 0.13.

		N_{Ef}	λ	ω_{log} (K)	T_c (K)
100 GPa	*P*4/*nmm*-Ca_2AsH_4	9.4	0.46	941	11 (7)
100 GPa	*Cc*-Ca_2AsH_6	8.9	0.70	241	16 (14)

At 100 GPa, the *P*4/*nmm*-Ca_2AsH_4 phase exhibits a λ of 0.49 and a ω_{log} of 941 K, resulting in a predicted T_c of 11 K. The *Cc*-Ca_2AsH_6 phase shows a λ of 0.70 and a ω_{log} of 241 K under the same pressure, yielding a T_c of 16 K. The larger λ value of *Cc*-Ca_2AsH_6 compared to *P*4/*nmm*-Ca_2AsH_4 at 100 GPa can be attributed primarily to the presence of H_2 units in the former, which often enhance λ.[46–48] Moreover, the Fermi surface nesting[49] in *Cc*-Ca_2AsH_6 is significantly stronger than that in *P*4/*nmm*-Ca_2AsH_4, as illustrated in Fig. S2. However, unlike H_3S[6] and LaH_{10},[3] the *Cc*-Ca_2AsH_6 phase exhibits an extremely low ω_{log}. In addition, both phases display λ values substantially smaller than those of H_3S and LaH_{10}.

Figure 5 presents the calculated phonon density of states (PHDOS), the Eliashberg spectral function $\alpha^2F(\omega)$, and the integrated EPC parameter $\lambda(\omega)$, which together elucidate the superconducting mechanisms in the Ca–As–H system. The phonon spectrum displays two distinctly separated frequency regions. Owing to the significant difference in atomic masses, vibrational modes below 500 cm^{-1} are primarily associated with the heavier Ca and As atoms, whereas modes above 500 cm^{-1} originate mainly from the lighter H atoms.

For *P*4/*nmm*-Ca_2AsH_4 at 100 GPa, the low-frequency vibrations are mainly due to the translational motion of Ca and As atoms. The vibrations in the 900–1200 cm^{-1} range, attributed to the rocking motion of H atoms, contribute approximately 49% to the total λ of this phase. The substantial contribution of mid-frequency hydrogen vibrations to the EPC is consistent with the behavior observed in covalent hydrides, such as H_3S,[50,51] PH_3,[52,53] and H_3Se.[38]

For *Cc*-Ca_2AsH_6 at 100 GPa, the low-frequency translational vibrations of Ca and As contribute 67% to λ, followed by mid-frequency rocking vibrations of H (800–1700 cm^{-1}), which account for approximately 30%. The high-frequency intramolecular stretching modes of H (> 1700 cm^{-1}) make only a minor contribution to λ. The phonon dispersion reveals extremely flat optical branches, particularly in the mid-to-high frequency regions, indicating highly localized vibrational modes with low group velocities. These flat phonon branches, though energetically high, exhibit weak dispersion and thus contribute less to ω_{log}. Due to its smaller ω_{log} compared with most hydrogen-rich compounds,[12,14] the T_c of this phase remains below 20 K. Nevertheless, the *Cc*-Ca_2AsH_6 phase benefits from its relatively larger λ, which compensates for the reduced ω_{log}, resulting in a T_c higher than that of the *P*4/*nmm*-Ca_2AsH_4 phase at 100 GPa.

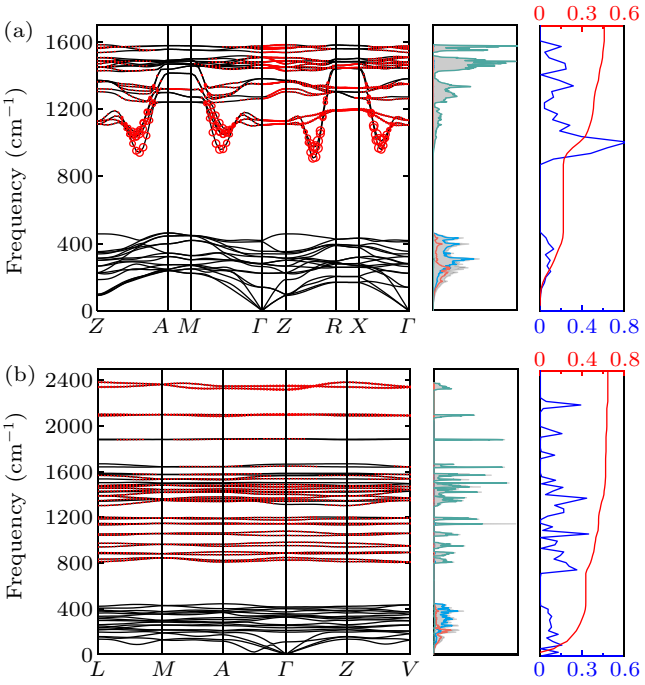


Fig. 5. Phonon dispersion relations, phonon densities of states, Eliashberg spectral functions $\alpha^2F(\omega)$, and electron–phonon coupling integrals $\lambda(\omega)$ for (a) *P*4/*nmm*-Ca_2AsH_4 and (b) *Cc*-Ca_2AsH_6 at 100 GPa. In the phonon spectra, the size of the red circles represents the strength of the electron–phonon coupling for each vibrational mode.

3. Conclusion

We systematically investigated the phase stability, electronic properties, and superconducting behavior of the Ca–As–H system under high-pressure conditions. Two thermodynamically stable hydrides, *P*4/*nmm*-Ca_2AsH_4 and *Cc*-Ca_2AsH_6, were identified at both 100 GPa and 200 GPa. Among them, the *P*4/*nmm*-Ca_2AsH_4 phase achieves a T_c of 11 K at 100 GPa, whereas the lower ω_{log} of *Cc*-Ca_2AsH_6 leads to a relatively moderate T_c of 16 K under the same pressure. Our findings demonstrate that Ca doping effectively lowers the stabilization pressure of binary As–H hydrides with higher hydrogen stoichiometry, thereby making them promising candidates for moderate-pressure superconductors.

Acknowledgments

This work was supported by the National Natural Science Foundation of China (Grant Nos. 12204280 and 12147135),

the Natural Science Foundation of Shandong Province (Grant No. ZR202103010004), the China Postdoctoral Science Foundation (Certificate Nos. 2023T160396 and 2021M691980), and the Youth Innovation Team Plan of Colleges and Universities in Shandong Province (Grant No. 2023KJ350).

References

[1] Bardeen J, Cooper L N and Schrieffer J R 1957 *Phys. Rev.* **106** 162
[2] Peng F, Sun Y, Pickard C J, Needs R J, Wu Q and Ma Y 2017 *Phys. Rev. Lett.* **119** 107001
[3] Liu H, Naumov I I, Hoffmann R, Ashcroft N W and Hemley R J 2017 *Proc. Natl. Acad. Sci. USA* **114** 6990
[4] Drozdov A P, Kong P P, Minkov V S, Besedin S P, Kuzovnikov M A, Mozaffari S, Balicas L, Balakirev F F, Graf D E, Prakapenka V B, Greenberg E, Knyazev D A, Tkacz M and Eremets M I 2019 *Nature* **569** 528
[5] Somayazulu M, Ahart M, Mishra A K, Geballe Z M, Baldini M, Meng Y, Struzhkin V V and Hemley R J 2019 *Phys. Rev. Lett.* **122** 027001
[6] Duan D, Liu Y, Tian F, Li D, Huang X, Zhao Z, Yu H, Liu B, Tian W and Cui T 2014 *Sci. Rep.* **4** 6968
[7] Drozdov A P, Eremets M I, Troyan I A, Ksenofontov V and Shylin S I 2015 *Nature* **525** 73
[8] Wang H, Tse J S, Tanaka K, Iitaka T and Ma Y 2012 *Proc. Natl. Acad. Sci. USA* **109** 6463
[9] Ma L, Wang K, Xie Y, Yang X, Wang Y, Zhou M, Liu H, Yu X, Zhao Y, Wang H, Liu G and Ma Y 2022 *Phys. Rev. Lett.* **128** 167001
[10] Troyan I A, Semenok D V, Kvashnin A G, *et al.* 2021 *Adv. Mater.* **33** 2006832
[11] Kong P, Minkov V S, Kuzovnikov M A, Drozdov A P, Besedin S P, Mozaffari S, Balicas L, Balakirev F F, Prakapenka V B, Chariton S, Knyazev D A, Greenberg E and Eremets M I 2021 *Nat. Commun.* **12** 5075
[12] Gao G, Wang L, Li M, Zhang J, Howie R T, Gregoryanz E, Struzhkin V V, Wang L and Tse J S 2021 *Mater. Today Phys.* **21** 100546
[13] Lilia B, Hennig R, Hirschfeld P, *et al.* 2022 *J. Phys.: Condens. Matter* **34** 183002
[14] Zhao W, Huang X, Zhang Z, Chen S, Du M, Duan D and Cui T 2023 *Natl. Sci. Rev.* **10** nwad307
[15] Sun Y, Lv J, Xie Y, Liu H and Ma Y 2019 *Phys. Rev. Lett.* **123** 097001
[16] Song Y, Bi J, Nakamoto Y, Shimizu K, Liu H, Zou B, Liu G, Wang H and Ma Y 2023 *Phys. Rev. Lett.* **130** 266001
[17] Wang S, Wu Z, Shen Z, Wang H, Li H, Li M, Zhang S, Song J, Liu Y, Gao G, Wang L and Tian Y 2025 *Phys. Rev. B* **111** 184106
[18] Fu Y, Du X, Zhang L, Peng F, Zhang M, Pickard C J, Needs R J, Singh D J, Zheng W and Ma Y 2016 *Chem. Mater.* **28** 1746
[19] Saha S, Di Cataldo S, Giannessi F, Cucciari A, Von Der Linden W and Boeri L 2023 *Phys. Rev. Mater.* **7** 054806
[20] Xu M, Duan D, Du M, Zhao W, An D, Song H and Cui T 2023 *Phys. Chem. Chem. Phys.* **25** 32534
[21] Chen H, Zhang W, Xue X and Lu W-C 2024 *Phys. B* **674** 415545
[22] Zhao J, Chen B, Li S, Chang Y, Yang X, Chen M and Li D 2025 *J. Mater. Chem. C* **13** 4128
[23] Zhu B, Shao D, Pei C, Wang Q, Wu J and Qi Y 2025 *Phys. Rev. B* **111**
[24] Wang Y, Lv J, Zhu L and Ma Y 2010 *Phys. Rev. B* **82** 094116
[25] Wang Y, Lv J, Zhu L and Ma Y 2012 *Comput. Phys. Commun.* **183** 2063
[26] Wu Q, Bergara A, Zhang X and Yang G 2025 *Phys. Rev. B* **111**
[27] Zhang J, Liu H, Chen C and Ma Y 2024 *Matter Radiat. Extrem.* **9** 037403
[28] Liang X, Wei X, Zurek E, Bergara A, Li P, Gao G and Tian Y 2024 *Matter Radiat. Extrem.* **9** 018401
[29] Li X, Guo Z, Zhang X and Yang G 2024 *Inorg. Chem.*
[30] Zhang J, Liu H, Ma Y and Chen C 2022 *Natl. Sci. Rev.* **9** nwab168
[31] Li X, Yang Q, Jin D, Ding S, Bergara A, Yao Y, Zhu L, Zhao J and Yang G 2025 *Phys. Rev. B* **111** 134111
[32] Fujihisa H, Nakamoto Y, Shimizu K, Yabuuchi T and Gotoh Y 2008 *Phys. Rev. Lett.* **101** 095503
[33] Yao Y, Klug D D, Sun J and Martoňák R 2009 *Phys. Rev. Lett.* **103** 055503
[34] Sakata M, Nakamoto Y, Shimizu K, Matsuoka T and Ohishi Y 2011 *Phys. Rev. B* **83** 220512
[35] Tsuppayakorn-aek P, Luo W, Ahuja R and Bovornratanaraks T 2018 *Sci. Rep.* **8** 3026
[36] Pickard C J and Needs R J 2007 *Nat. Phys.* **3** 473
[37] Shao Z, Duan D, Ma Y, Yu H, Song H, Xie H, Li D, Tian F, Liu B and Cui T 2019 *Inorg. Chem.* **58** 2558
[38] Zhang S, Wang Y, Zhang J, Liu H, Zhong X, Song H-F, Yang G, Zhang L and Ma Y 2015 *Sci. Rep.* **5** 15433
[39] Wu J, Zhao L, Chen H, Wang D, Chen J, Guo X, Zang Q and Lu W 2018 *Phys. Status Solidi B* **255** 1800224
[40] Liang X, Bergara A, Wang L, Wen B, Zhao Z, Zhou X-F, He J, Gao G and Tian Y 2019 *Phys. Rev. B* **99** 100505
[41] Song H, Zhang Z, Du M, Jiang Q, Duan D and Cui T 2021 *Phys. Rev. B* **104** 104509
[42] Wang J, Deng S, Liu Z and Liu Z 2015 *Natl. Sci. Rev.* **2** 22
[43] Checkelsky J G, Bernevig B A, Coleman P, Si Q and Paschen S 2024 *Nat. Rev. Mater.* **9** 509
[44] Shao Z, Duan D, Ma Y, Yu H, Song H, Xie H, Li D, Tian F, Liu B and Cui T 2019 *npj Comput. Mater.* **5** 104
[45] Li B, Yang Y, Fan Y, Zhu C, Liu S and Shi Z 2023 *Chin. Phys. Lett.* **40** 097402
[46] Chen W, Semenok D V, Kvashnin A G, Huang X, Kruglov I A, Galasso M, Song H, Duan D, Goncharov A F, Prakapenka V B, Oganov A R and Cui T 2021 *Nat. Commun.* **12** 273
[47] Chen B, Conway L J, Sun W, Kuang X, Lu C and Hermann A 2021 *Phys. Rev. B* **103** 035131
[48] Yu J, Yong X, Liu H and Lu S 2024 *Phys. Rev. B* **110** 224507
[49] Li C, Ravichandran N K, Lindsay L and Broido D 2018 *Phys. Rev. Lett.* **121** 175901
[50] Duan D, Huang X, Tian F, Li D, Yu H, Liu Y, Ma Y, Liu B and Cui T 2015 *Phys. Rev. B* **91** 180502
[51] Einaga M, Sakata M, Ishikawa T, Shimizu K, Eremets M I, Drozdov A P, Troyan I A, Hirao N and Ohishi Y 2016 *Nat. Phys.* **12** 835
[52] Durajski A P 2016 *Sci. Rep.* **6** 38570
[53] Liu H, Li Y, Gao G, Tse J S and Naumov I I 2016 *J. Phys. Chem. C* **120** 3458